Journal of Photochemistry and Photobiology A: Chemistry 216 (2010) 149–155

Contents lists available at ScienceDirect

Journal of Photochemistry and Photobiology A: Chemistry

journal homepage: www.elsevier.com/locate/jphotochem

Surface modification of ZnO with Ag improves its photocatalytic efficiency and photostability

Wei Xie, Yuanzhi Li*, Wei Sun, Jichao Huang, Hao Xie, Xiujian Zhao

Key Lab. of Silicate Materials Science and Engineering (Wuhan University of Technology), Ministry of Education, 122 Luoshi Road, Wuhan 430070, China

ARTICLE INFO

Article history:
Available online 6 July 2010

Keywords:
ZnO
Silver
Photocatalytic
Photostability
O_2 chemisorption

ABSTRACT

Ag/ZnO photocatalysts with different Ag loadings were prepared by photocatalytic reduction of Ag^+ on ZnO with ethanol as hole scavenger. It was found that loading an appropriate amount of Ag on ZnO not only enhances its photocatalytic activity, but also improves its photostability. The Ag/ZnO photocatalysts were characterized with XRD, BET, DRUV–vis, Raman, PL, and photoelectrochemical measurement. No matter what the Ag loading is higher or low, silver exists in the form of metallic species in the Ag/ZnO photocatalysts. The enhancement of photocatalytic activity is due to the fact that the modification of ZnO with an appropriate amount of Ag can increase the separation efficiency of photogenerated electrons and holes in ZnO, and the improvement of photostability of ZnO is attributed to a considerable decrease of the surface defect sites of ZnO after the Ag loading. The chemisorption of molecular oxygen and the chemisorption of atomic oxygen on Ag in the Ag/ZnO photocatalysts were observed. It was found that the metallic Ag in the Ag/ZnO photocatalysts does play a new role of O_2 chemisorption sites except for electron acceptor, by which chemisorbed molecular oxygen reacts with photogenerated electrons to form active oxygen species, and thus facilitates the trapping of photogenerated electrons and further improves the photocatalytic activity of the Ag/ZnO photocatalysts.

1. Introduction

Heterogeneous photocatalysis based on nanostructured TiO_2 has been extensively studied as an important destructive technology leading to the total mineralization of a wide range of organic dyes, which has been being an international hot topic for decades. ZnO is another semiconductor investigated as a potential photocatalyst in recent years. Various kinds of nanostructured ZnO, such as nanoparticle, nanorod, nanobelt, nanoplate, hollow sphere, and micro/nanostructure, have been used for the photodegradation of dye pollutants [1–6]. In some cases, ZnO exhibits a better photocatalytic efficiency than TiO_2 [6,7] due to its higher efficiency of generation, mobility, and separation of photoinduced electrons and holes [8].

One of the major drawbacks of ZnO photocatalyst is its photoinstability in aqueous solution due to its photocorrosion with UV irradiation, which significantly decreases the photocatalytic activity of ZnO and blocks its practical application in environment purification [9]. It is anticipated that ZnO would become an excellent photocatalyst if the photocorrosion could be greatly suppressed. Several methods have been developed to improve its photostability, including surface organic coating of ZnO [10], and surface hybridization of ZnO with carbon and fullerenes C_{60} [11,12]. These works provided possibility for the practical application of ZnO in the photocatalytic removal of dye pollutants. Recently, we found that microscale ZnO exhibited much better photostability than nano-ZnO due to its better crystallinity and lower defects. The photostability of the microscale ZnO is further improved by the surface modification of ZnO with a small amount of TiO_2 [8]. However, the photostability improvement of ZnO with TiO_2 modification is at the cost of the slight decrease of its photocatalytic activity. In our another recent work, it was found that the formation of the surface complex between phenolic compounds and ZnO results in the substantial improvement of the photostability of ZnO as it leads to a considerable decrease of the surface defect sites of ZnO [13]. However, the photostability improvement of ZnO induced by the surface complex is only workable in the special cases. Therefore, it is still of great challenge to improve both photocatalytic activity and the photostability of ZnO by more general and inexpensive approaches.

Enlightened by a lot of studies of the beneficial role of metallic Ag nanoparticles deposited on TiO_2 for improving the photocatalytic efficiency of nanostructured TiO_2 [14–16], many researchers reported that depositing Ag on various nanostructured ZnO boosts its photocatalytic activity [17–25]. It is widely accepted that Ag nanoparticles on ZnO acting as electron sinks can trap the photogenerated electrons from the semiconductor and thus improve the separation efficiency of photogenerated electrons and holes,

* Corresponding author. Tel.: +86 27 87651856; fax: +86 27 87883743.
E-mail address: liyuanzhi66@hotmail.com (Y. Li).

1010-6030/$ – see front matter © 2010 Elsevier B.V. All rights reserved.
doi:10.1016/j.jphotochem.2010.06.032

which results in the improvement of the photocatalytic activity of ZnO. However, whether the Ag modification could improve the photostability of ZnO has not been reported.

In this article, we found that loading an appropriate amount of Ag on ZnO not only enhances its photocatalytic activity, but also improves its photostability. Further, it was found for the first time that the metallic Ag in the Ag/ZnO photocatalysts does play another role of O_2 chemisorption sites except for electron acceptor, by which chemisorbed molecular oxygen reacts with photogenerated electrons to form active oxygen species, and thus facilitates the trapping of photogenerated electrons and further improves the photocatalytic activity of the Ag/ZnO photocatalysts.

2. Experimental

2.1. Materials

Microscale ZnO was purchased from Wuhan Zhongbei Chemical Reagent Co. $AgNO_3$, poly(ethylene glycol), crystal violet (CV), ethanol, and methanol were purchased from Shanghai Chemical Co. All of these chemicals were used without further purification.

2.2. Preparation of photocatalysts and photoelectrode

1.0 g of the microscale ZnO powder was added to 100 mL of distilled water in the beaker. A known amount of 0.2 mol L^{-1} $AgNO_3$ and 2 mL of ethanol were added to the obtained suspension. The suspension was illuminated by a 125 W high pressure Hg lamp (Shanghai Yaming Lighting Appliance Co. Ltd., thereafter denoted as UV lamp) for 2 h under magnetic stirring. The mixture was filtered, washed thoroughly with distilled water, and dried at 100 °C for 2 h.

A mixture of the photocatalyst powder and poly(ethylene glycol) with a weight ratio of 5% was added to 15 mL of ethanol and ultrasonicated for 30 min. The obtained mixture was uniformly spread on an ITO glass substrate. After the evaporation of ethanol, the sample was heated to 480 °C in a muffle furnace at a rate of 2 °C min^{-1} and remained at this temperature for 2 h to completely remove poly(ethylene glycol).

2.3. Characterization

X-ray diffraction (XRD) patterns were obtained on a Rigaku D/Max-IIIA X-ray diffractometer. The Brunauer–Emmett–Teller (BET) surface area was measured on Autosorb-1 using N_2 adsorption at −196 °C for the sample predegassed at 200 °C in a vacuum for 2 h. Diffusive reflectance UV–vis (DRUV–vis) absorption spectra were recorded on an UV-2550 spectrophotometer. Raman spectra were recorded on a Renishaw inVia Raman microscope with an excitation of 514.5 nm laser light. Photoluminescence (PL) spectra were recorded at room temperature on a Shimadzu RF-5301 PC spectrometer using 320 nm excitation light.

Photoelectrochemical measurements were carried out by using a homemade three-electrode quartz cell, Pt wire as the counter electrode, a saturated Ag/AgCl electrode as the reference electrode, and the thin film of the photocatalysts on ITO as the working electrode on an electrochemical analyzer (CHI750). The electrolyte used was a solution of 0.2 mol L^{-1} Na_2SO_4. A 125 W high pressure Hg Lamp (maximum wavelength: 385 nm, Shanghai Yaming Lighting Appliance Co. Ltd., thereafter denoted as UV lamp) was used as light source. Before the measurement, the electrolyte was purged by highly pure N_2 to remove the dissolved oxygen.

2.4. Photocatalytic activity

The photocatalytic activity of the photocatalysts was evaluated by the photodegradation of CV. The light source was a UV lamp. The reaction was maintained at ambient temperature. In a typical experiment, aqueous suspensions of dye (50 mL, 1×10^{-4} mol L^{-1}) and 0.2000 g of the photocatalyst powder were placed in the beaker. Prior to irradiation, the suspension was magnetically stirred in the dark to ensure the establishment of an adsorption/desorption equilibrium. The suspension was kept under constant air-equilibrated condition. At the intervals of given irradiation time, 1.0 mL of the suspension was collected and centrifuged to remove the particles. The dye concentration was determined by measuring the UV–vis absorbance of the dye aqueous solution.

2.5. Detection of hydroxyl radicals

The experimental procedure for the detection of hydroxyl radicals were as follows: 0.2000 g of Ag/ZnO powder was dispersed in a 50 mL aqueous solution of 1.0×10^{-4} mol L^{-1} terephthalic acid and 4×10^{-4} mol L^{-1} NaOH in a beaker at ambient temperature. An UV lamp was used as a light source. At the intervals of given irradiation time, 1 mL of the suspension was collected and centrifuged to remove the particles. PL spectra of the 2-hydroxyterephthalic acid produced by the reaction between terephthalic acid and photogenerated hydroxyl radicals were recorded on a Shimadzu RF-5301 PC spectrometer using 315 nm excitation light.

3. Results and discussion

3.1. XRD

The Ag/ZnO photocatalysts were prepared by photocatalytic reduction of Ag^+ on ZnO with ethanol as hole scavenger. Upon UV irradiation, electrons in the valence band of ZnO are excited to its conduction band with simultaneous generation of the same amount of holes left behind. Ag^+ ions in aqueous solution are reduced by the photogenerated electrons and deposited on the surface of ZnO while the holes are captured by ethanol. Fig. 1 shows XRD patterns of the pure ZnO and Ag/ZnO photocatalysts with different Ag loadings. The observed diffraction peaks of the pure ZnO catalyst can be indexed to those of hexagonal wurtzite ZnO (JCPDS 89-0511). No impurity phases were detected. Its average crystal size is determined to be 353 nm according to Scherrer formula ($L = 0.89\lambda/\beta\cos\theta$). Its BET surface area is 3.0 m^2 g^{-1}. As can be seen from Fig. 1, after loading Ag on the ZnO catalyst, no detectable structural change is observed for the ZnO catalyst, which suggests that the surface modification does not change the bulk intrinsic property of the ZnO photocatalyst. For the Ag/ZnO photocatalysts with higher Ag loading (≥1.0 wt%), crystalline metallic Ag is observed by XRD. However, in the case of lower Ag loading

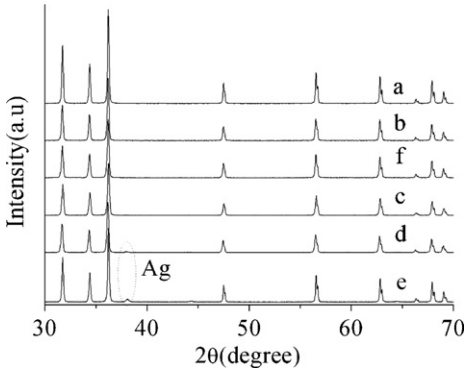

Fig. 1. XRD patterns of the Ag/ZnO photocatalysts with different Ag loadings: (a) pure ZnO, (b) 0.04 wt%Ag/ZnO, (c) 0.2 wt%Ag/ZnO, (d) 1.0 wt%Ag/ZnO, (e) 6.7 wt%Ag/ZnO and (f) the 0.2 wt%Ag/ZnO after recycled for eight times for the photodegradation of CV.

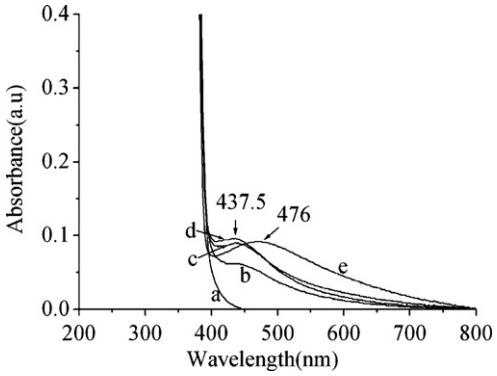

Fig. 2. DRUV–vis spectra of the Ag/ZnO photocatalysts with different Ag loadings: (a) pure ZnO, (b) 0.04 wt%Ag/ZnO, (c) 0.2 wt%Ag/ZnO, (d) 1.0 wt%Ag/ZnO and (e) 6.7 wt%Ag/ZnO.

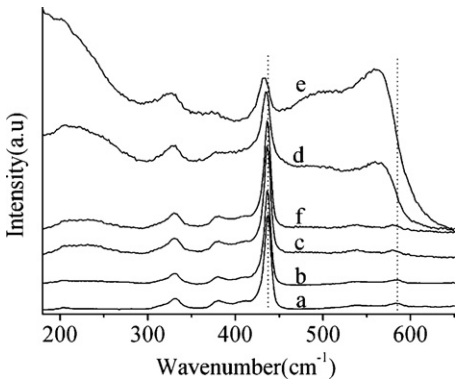

Fig. 3. Raman spectra of the Ag/ZnO photocatalysts with different Ag loadings: (a) pure ZnO, (b) 0.04 wt%Ag/ZnO, (c) 0.2 wt%Ag/ZnO, (d) 1.0 wt%Ag/ZnO, (e) 6.7 wt%Ag/ZnO and (f) the 0.2 wt%Ag/ZnO after recycled for eight times for the photodegradation of CV.

(≤0.2 wt%), crystalline metallic Ag is not detected by XRD in the Ag/ZnO photocatalysts, implying small Ag nanoparticles that are highly dispersed on the surface of ZnO.

3.2. DRUV–vis

Fig. 2 presents DRUV–vis spectra of the pure ZnO and Ag/ZnO photocatalysts with different Ag loadings. All of the Ag/ZnO photocatalysts exhibit absorption band in the region of 400–800 nm, which is attributed to the characteristic absorption of surface plasmon resulting from the metallic Ag clusters and/or nanoparticles in the Ag/ZnO photocatalysts [17]. This observation reveals that even in the Ag/ZnO photocatalysts with low Ag loading (0.04%Ag/ZnO and 0.2%Ag/ZnO), Ag also exists in the form of metallic species that are highly dispersed on the surface of the ZnO catalyst. When the Ag loadings are below 1.0%, although the absorption of the Ag surface plasmon increases with the evolution of the Ag loading, their maximum absorption almost remained unchanged (around 437.5 nm). In contrast, increasing the Ag loadings to 6.7% leads to a red shift of 38.5 nm for the maximum absorption of the Ag surface plasmon. The plasmon absorption of silver is represented by the following equation [26]:

$$\lambda_p = \left[\frac{4\pi^2 c^2 m_{eff}\epsilon_0}{Ne^2}\right]^{1/2}$$

where m_{eff} is the effective mass of the free electron of the metal and N is the electron density of the metal. The position of plasmon absorption is related to the electron density of the metal. With the decrease of the electron density of the metal, the plasmon absorption λ_p of metal was increased, which results in the red shift of the plasmon absorption band. The red shift of the plasmon peak of silver in the 6.67%Ag/ZnO photocatalyst compared with the Ag/ZnO photocatalysts with lower Ag loading suggests that the electron density of Ag was decreased. The decrease of electron density of Ag is due to the chemisorption of atomic oxygen on the surface of Ag, which will be discussed thereinafter.

3.3. Raman

Fig. 3 shows the Raman spectra of the Ag/ZnO photocatalysts with different Ag loadings. The pure ZnO photocatalyst exhibits strong bands at 583.1, 537.8, 435.3, 382.0, and 331.6 cm^{-1}, which are attributed to the E_1(LO), A_1(LO), E_2, A_1(TO), and A_1 modes of wurtzite ZnO, respectively [27]. In the case of lower Ag loading (≤0.2%), no detectable change for the E_1(LO), A_1(LO), E_2, A_1(TO), and A_1 modes of ZnO is observed after the Ag loading. When the Ag loading is above 1.0%, the E_2 and E_1(LO) modes have an obvious blue shift of 3.4 and 25 cm^{-1}, respectively. Actually, it is observed by carefully checking the Raman spectra of the Ag/ZnO photocatalysts with lower Ag loading that the E_1(LO) mode exhibits a slight blue shift with increasing Ag loading. The much larger blue shift of the E_1(LO) mode than the E_2 mode suggests that the E_1(LO) mode is more sensitive to the surface modification of ZnO with Ag. More interestingly, when the Ag loading is above 1.0%, the absorption of E_1(LO) mode is greatly enhanced. This surface enhancement Raman spectra (SERS) is most probably due to the local field enhancement induced by the surface plasmons of the metallic Ag on the surface of the Ag/ZnO photocatalysts [25]. As E_1(LO) mode is associated with oxygen deficiency [28,29], the results reveal that the metallic Ag deposits around the sites of oxygen vacancy on the surface of the Ag/ZnO photocatalysts, which is very important for improving the photostability of ZnO (discussed thereinafter).

It is interestingly observed that there is a broad band around 225 cm^{-1} after the Ag loading, which is attributed to the $\nu(Ag–O_2)$ of molecular oxygen species chemisorbed on defects of the metallic Ag [30–32]. With the evolution of the Ag loading from 0.2% to 1.0% to 6.7%, the intensity of the broad band increases, indicating that more molecular oxygen species are chemisorbed on defects of the metallic Ag. When the Ag loading is above 1.0%, there is another weak broadband around 485 cm^{-1}, which is ascribed to the ν(Ag–O) of atomic oxygen surface chemisorbed on defects of the metallic Ag [30,32]. The enhanced chemisorption of molecular oxygen species and the chemisorption of atomic oxygen on Ag lead to the decrease of the electron density of the metallic Ag in the 1.0%Ag/ZnO and 6.7%Ag/ZnO photocatalysts, which results in the red shift of the plasmon absorption band as observed in the above DRUV–vis spectra [26].

3.4. Photocatalytic activity

Dye effluents from textile industries are becoming a serious environmental problem because of their unacceptable color, high chemical oxygen demand content, and resistance to chemical, photochemical, and biological degradation. We chose photodegradation of CV as model dye with UV irradiation to evaluate the photocatalytic activity of the photocatalysts. Fig. 4 shows the time course of the decrease in the concentration of CV under UV irradiation. As can be seen from Fig. 4, compared with the pure ZnO, loading a small amount of Ag on ZnO (0.04 wt%) leads to the enhancement of its photocatalytic activity. When the Ag loading increases to 0.2%, its photocatalytic activity reaches to maximum. When the Ag loading is 1.0%, its photocatalytic activity is almost similar to that of the 0.2%Ag/ZnO photocatalyst. Further increasing

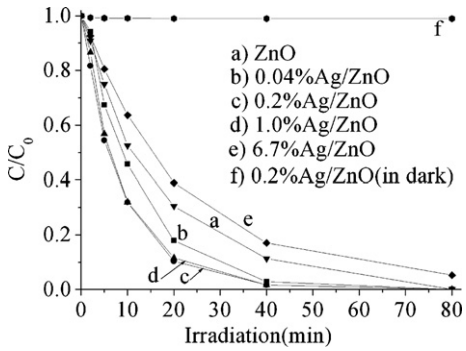

Fig. 4. The time course of the decrease in the concentration for the photodegradation of CV under UV irradiation.

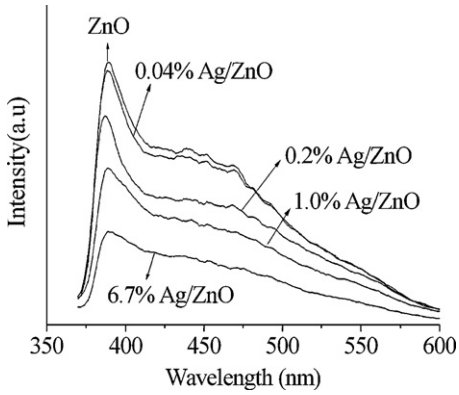

Fig. 6. The room temperature photoluminescence spectra with excitation at 320 nm for the photocatalysts.

the Ag loading to 6.7% results in a decrease of its photocatalytic activity.

3.5. Photostability

The recycled experiments for the photodegradation of CV under UV irradiation were performed to evaluate the photostability of the 0.2%Ag/ZnO photocatalysts. As shown in Fig. 5, the pure ZnO photocatalyst suffers from a gradual deactivation in the process of recycling. After recycled for eight times, its photocatalytic conversion decreases to 46.7%. In contrast, the 0.2%Ag/ZnO photocatalyst exhibits much better photostability than the pure ZnO photocatalyst. Its photocatalytic activity almost remained unchanged after 8 cycles. The recycled 0.2%Ag/ZnO photocatalyst was gained from the suspension by a simple filtration, and then was characterized by XRD and Raman. As shown in Figs. 1 and 3, both its XRD pattern and Raman spectra are almost identical to those of the fresh 0.2%Ag/ZnO photocatalyst. This observation indicates that the structure of the 0.2%Ag/ZnO photocatalyst remains unchanged after recycled for eight times, which can give an reasonable explanation to the fact why the 0.2%Ag/ZnO photocatalyst exhibits very good photostability. It has been reported that the photocatalytic activity of ZnO can be enhanced by the modification of ZnO with Ag [17–25]. In our case, it was found for the first time that the modification of ZnO with Ag not only enhances the photocatalytic activity of ZnO, but also improves the photostability of ZnO.

One of the major drawbacks of nanosized photocatalysts for their application in treating wastewater is the special difficulty in separation from a suspension due to their nanosized particle dimension, which in turn significantly increases the running cost, and sometimes even produces a secondary pollution. To solve the problem, much effort has been focused on forming a composite with magnetite [33], which usually leads to the decrease of their photocatalytic efficiency. The high photocatalytic activity and very good photostability of the 0.2%Ag/ZnO photocatalyst together with their easy separation from a suspension by conventional technology of filtration will facilitate their application in wastewater treatment.

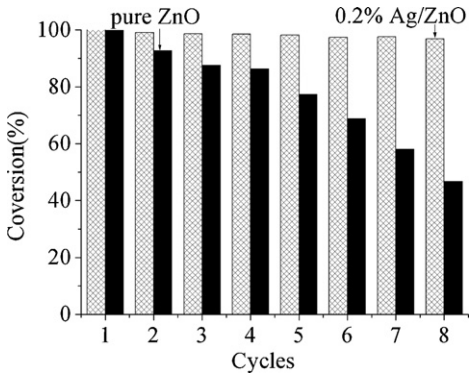

Fig. 5. The durability of the photocatalysts for the photodegradation of CV under UV irradiation.

3.6. Photoluminescence

In a photocatalytic process, the separation and recombination of photoinduced electron and hole are competitive pathways, and photocatalytic activity is effective when the recombination is prevented. The extent of recombination can be probed by the intensity of photoluminescence. It is well-known that the photoluminescent property of ZnO is sensitive to its defects [34,35]. A strong UV emission at 390 nm and several relatively weak visible emissions in the range of 400–580 nm are observed for the pure ZnO photocatalyst (Fig. 6). The UV emission is attributed to free excitonic emission near band edge. The visible emissions are due to transition in various kinds of defect states [34,35]. Compared with the pure ZnO, loading Ag on ZnO leads to a decrease of both the UV and visible emissions. With the evolution of the Ag loading from 0.04% to 6.7%, both the UV and visible emissions of the Ag/ZnO photocatalyst rapidly decrease. The decrease of the UV emission for the Ag/ZnO photocatalyst can be ascribed to the electron trapping effect of Ag, which acts as electron acceptor, thus hindering the recombination of charge carriers on ZnO [23]. The electron trapping effect of Ag is favorable for the improvement of the photocatalytic activity of ZnO due to the enhancement of the separation efficiency of photogenerated electrons and holes. The considerable decrease of the visible emissions indicates that the surface defects in the ZnO photocatalyst are greatly reduced after the Ag loading, suggesting that the metallic Ag is deposited on the defect sites, which is in agreement to the results obtained by Raman spectra.

The photocorrosion of ZnO consists of two slow steps where two holes are trapped on the surface of ZnO, followed by the fast formation of an oxygen molecule and the fast expulsion of Zn^{2+} from the surface, and the overall reaction may be represented as: $ZnO + 2h^+ \rightarrow Zn^{2+} + 0.5O_2$ [12,36]. Very recently, it was found by Kislov et al. [37] that the photocorrosion mainly occurs in the surface defect sites of ZnO. Zhu et al. achieved a photostable hybrid photocatalyst of C_{60}/ZnO by anchoring fullerenes C_{60} molecule on the surface defect sites of ZnO, which substantially reduced the activation of surface oxygen atom, and effectively inhibited the photocorrosion of ZnO [14]. In our case, loading 0.2% of Ag on ZnO results in a considerable decrease of the surface defect sites of ZnO, which inhibits the photocorrosion of ZnO and thus improves its photostability.

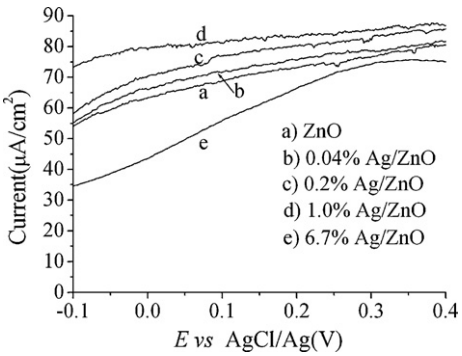

Fig. 7. The photoelectrochemical response of the pure ZnO and Ag/ZnO composite electrodes vs bias potential under UV irradiation.

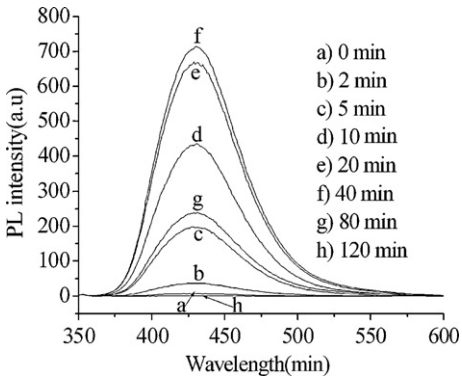

Fig. 8. The time course of fluorescence spectral changes with excitation at 315 nm under UV irradiation in the suspension of 0.2000 g of 0.2%Ag/ZnO photocatalyst and 50 mL of 1.0×10^{-4} mol L^{-1} aqueous basic solution of terephthalic acid.

The lowest UV PL emission for the 6.7%Ag/ZnO photocatalyst suggests that the recombination of photogenerated electrons and holes through radiative pathway is greatly inhibited. It seems that the 6.7%Ag/ZnO photocatalyst should exhibit best photocatalytic activity. However, the photocatalysts shows lowest photocatalytic activity among the Ag/ZnO photocatalysts. Therefore, more experimental data is needed to study the contradiction against the expectation.

3.7. Photoelectrochemical property

Compared with the PL results, the photocurrent measurement can give more direct evidence for the separation efficiency of photogenerated electrons and holes in the photocatalysts. Under UV irradiation, the electron in the valence band of ZnO can be excited to their corresponding conduction band, thus, the efficient separation of photoinduced electrons and holes leads to the generation of photocurrent. As can be seen from Fig. 7, compared with the pure ZnO photocatalyst, loading a small amount of Ag on ZnO leads to an enhancement of its photocurrent. With the evolution of the loading amount of Ag from 0.04% to 0.2% to 1.0%, the photocurrent of the Ag/ZnO photocatalyst gradually increases. This result indicates that the modification of ZnO with an appropriate amount of Ag can increase the separation efficiency of photogenerated electrons and holes in ZnO, which results in the enhancement of its photocatalytic activity. However, further increasing the Ag loading to 6.7% results in a considerable decrease of its photocurrent. This observation reveals that the existence of the excess Ag decreases the separation efficiency of photogenerated electrons and holes in the 6.7%Ag/ZnO photocatalyst because the possibility of hole capture increases by large number of negatively charged Ag particles on ZnO when the Ag loading is above its optimum [38]. This process of hole capture probably proceeds in nonradiative pathway, which could not be detected by conventional PL measurement. Therefore, the lowest photocatalytic activity of the 6.7%Ag/ZnO photocatalyst is attributed to its lowest separation efficiency of photogenerated electrons and holes.

3.8. Mechanism and role of Ag

To reveal the active species involved in the photodegradation process of the Ag/ZnO photocatalyst, the formation of hydroxyl radicals (•OH) on the surface of the Ag/ZnO photocatalyst under UV irradiation was detected by the PL technique using terephthalic acid as a probe molecule, which readily reacts with •OH to produce highly fluorescent product, 2-hydroxyterephthalic acid. The PL intensity of 2-hydroxyterephtalic acid at 425 nm is proportional to the amount of •OH produced on the surface of the Ag/ZnO photocatalyst [39–41]. Fig. 8 presents the time course of fluorescence spectral changes with excitation at 315 nm under UV irradiation in the suspension of the 0.2%Ag/ZnO photocatalyst and aqueous basic solution of terephthalic acid. As shown in Fig. 8, in the initial 40 min, the PL intensity around 425 nm increases with the evolution of UV irradiation time, which demonstrates the production of hydroxyl radicals on the surface of the Ag/ZnO photocatalyst with UV irradiation [39–41]. After that, further increasing UV irradiation time leads to a quick decrease of the PL intensity around 425 nm, which indicates that the concentration of the produced 2-hydroxyterephthalic acid quickly decreases. These observations reveal that the photodegradation of terephthalic acid proceeds in two continuous steps as following: terephthalic acid first reacts with the photogenerated hydroxyl radicals to form 2-hydroxyterephthalic acid, and then the produced 2-hydroxyterephthalic acid is further oxidized by the hydroxyl radicals.

To reveal whether the active oxygen species formed by the reaction between O_2 (e.g. chemisorbed O_2, physisorbed O_2, and O_2 dissolved in the dye solution) and the photogenerated electrons make a contribution to the photodegradation of CV, methanol was used as hole scavenger [42,43] in the photodegradation of CV (50 mL, 1×10^{-4} mol L^{-1}). Fig. 9 shows the time course of the decrease in the concentration of CV in the presence of excess methanol (0.99 mol L^{-1}) and the 0.2%Ag/ZnO photocatalyst under UV irradiation. As can be seen from Fig. 9, in the absence of the 0.2%Ag/ZnO photocatalyst, only 9.0% of CV is photodegraded in the presence of excess methanol under UV irradiation within 2 h. In contrast, 46.7% of CV is photodegraded in the presence of excess methanol and the 0.2%Ag/ZnO photocatalyst under UV irradiation within 2 h. This observation reveals that CV can be photodegraded by the active oxygen species formed by the reaction between O_2 and the photogenerated electrons.

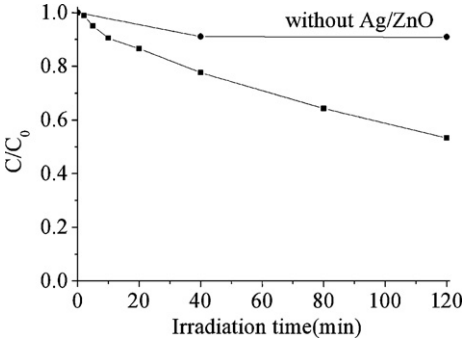

Fig. 9. The time course of the decrease in the concentration of CV in the presence of excess methanol (0.99 mol L^{-1}) and the 0.2%Ag/ZnO photocatalyst under UV irradiation.

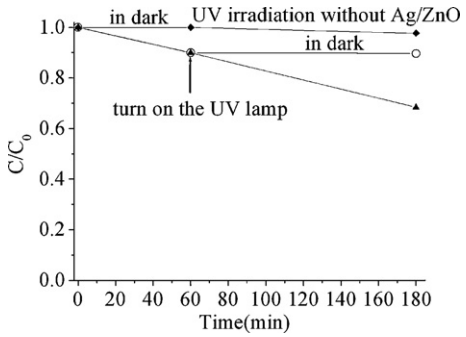

Fig. 10. The time course of the decrease in the concentration of CV using the 0.2%Ag/ZnO sample as photocatalyst in the flow of high pure Ar under UV irradiation.

The above obtained results suggest that the mechanism for the photodegradation of CV on the Ag/ZnO photocatalyst is as follows: Upon UV irradiation, electrons are excited from the valence band of ZnO to its conduction band, leaving the corresponding holes in the valence band. The electrons further transfer to Ag in the Ag/ZnO photocatalyst, and thus the separation efficiency of the photoinduced electrons and holes is enhanced. The photogenerated holes in the valence band of ZnO react with hydroxyl groups to form hydroxyl radicals, which lead to the photocatalytic oxidation of the dye. At the same time, the photogenerated electrons react with O_2 to form active oxygen species, which also participate in the photocatalytic oxidation of the dye. This mechanism proposed on the basis of the experimental evidences is in agreement with that proposed in the literatures [17,23,24].

As observed by Raman, O_2 is chemisorbed on Ag in the Ag/ZnO photocatalysts. Under UV irradiation, the photogenerated electrons trapped by the metallic Ag in the Ag/ZnO photocatalysts either reacts with the chemisorbed O_2 or reacts with O_2 physisorbed on Ag and O_2 dissolved in the dye solution to form active oxygen species. Obviously, the former reaction is more favorable than the latter reaction because of its lower activation energy. To confirm whether the active oxygen formed by the reaction between the chemisorbed O_2 and the photogenerated electrons takes part in the photodegradation of CV, the photodegradation of CV in the absence of O_2 physisorbed on Ag and O_2 dissolved in the dye solution was tested. In order to do this experiment, the aqueous suspension of dye (50 mL, 1×10^{-4} mol L^{-1}) and 0.2000 g of the 0.2%Ag/ZnO photocatalyst in a beaker was placed on the bottom of a closed stainless reactor (7.2 L) with quartz window on the upper cover that was connected to a high pure Ar cylinder through a valve and stainless pipeline, of which the another end was immersed in the suspension. This setup can guarantee a complete separation of the suspension in the beaker from air. The suspension was purged with Ar in the flow of highly pure Ar in dark for 1 h to remove O_2 physisorbed on Ag and O_2 dissolved in the dye solution and ensure the establishment of an adsorption/desorption equilibrium of CV on the photocatalyst, and then the photodegradation of CV was started by turning on the UV lamp. Fig. 10 presents the time course of the decrease in the concentration of CV using the 0.2%Ag/ZnO sample as photocatalyst in the flow of high pure Ar under UV irradiation. As can be seen from Fig. 10, in the absence of the 0.2%Ag/ZnO photocatalyst, CV cannot be photodegraded in the flow of high pure Ar under UV irradiation. However, the concentration of CV slowly decreases in the presence of the 0.2%Ag/ZnO photocatalyst in the flow of high pure Ar with the evolution of UV irradiation time. After 2 h, 21.6% of CV is photodegraded. The photodegradation of CV in the absence of dissolved O_2 in the dye solution and physisorbed O_2 indicates that CV can be photodegraded by the active oxygen species formed by the reaction between the photogenerated electrons and O_2 chemisorbed on the metallic Ag in the 0.2%Ag/ZnO photocatalyst. This result reveals that the metallic Ag in the Ag/ZnO photocatalyst does play another role of O_2 adsorption sites except for electron acceptor, by which chemisorbed molecular oxygen reacts with photogenerated electrons to form active oxygen species, and thus facilitates the trapping of photogenerated electrons by reducing the back electron transfer from Ag to ZnO and further improves the photocatalytic activity of the Ag/ZnO photocatalysts.

4. Conclusions

In summary, Ag/ZnO photocatalysts with different Ag loadings were prepared by photocatalytic reduction of Ag^+ on ZnO with ethanol as hole scavenger. We found that loading an appropriate amount of Ag on ZnO not only enhances its photocatalytic activity, but also improves its photostability. The enhancement of photocatalytic activity is due to the fact that the modification of ZnO with an appropriate amount of Ag can increase the separation efficiency of photogenerated electrons and holes in ZnO, and the improvement of photostability of ZnO is attributed to a considerable decrease of the surface defect sites of ZnO after the Ag loading. It was found that the metallic Ag in the Ag/ZnO photocatalysts does play two new roles of O_2 chemisorption sites except for electron acceptor, by which chemisorbed molecular oxygen reacts with photogenerated electrons to form active oxygen species, and thus facilitates the trapping of photogenerated electrons and further improves the photocatalytic activity of the Ag/ZnO photocatalysts.

Acknowledgements

This work was supported by National Basic Research Program of China (2009CB939704), Important Project of Ministry of Education of China (309021), Scientific Research Foundation for the Returned Overseas Chinese Scholars ([2008] 890), and Nippon Sheet Glass Foundation.

References

[1] E.S. Jang, J.H. Won, S.J. Hwang, J.H. Choy, Fine tuning of the face orientation of ZnO crystals to optimize their photocatalytic activity, Adv. Mater. 18 (2006) 3309–3312.
[2] T.J. Sun, J.S. Qiu, C.H. Liang, Controllable fabrication and photocatalytic activity of ZnO nanobelt arrays, J. Phys. Chem. C 112 (2008) 715–721.
[3] C.H. Ye, Y. Bando, G.Z. Shen, D. Golberg, Thickness-dependent photocatalytic performance of ZnO nanoplatelets, J. Phys. Chem. B 110 (2006) 15146–15151.
[4] J.G. Yu, X.X. Yu, Hydrothermal synthesis and photocatalytic activity of zinc oxide hollow spheres, Environ. Sci. Technol. 42 (2008) 4902–4907.
[5] Z.W. Deng, M. Chen, G.X. Gu, L.M. Wu, A facile method to fabricate ZnO hollow spheres and their photocatalytic property, J. Phys. Chem. B 112 (2008) 16–22.
[6] F. Lu, W.P. Cai, Y.G. Zhang, ZnO hierarchical micro/nanoarchitectures: solvothermal synthesis and structurally enhanced photocatalytic performance, Adv. Funct. Mater. 18 (2008) 1047–1056.
[7] S. Sakthivel, B. Neppolian, M.V. Shankar, B. Arabindoo, M. Palanichamy, V. Murugesan, Solar photocatalytic degradation of azo dye: comparison of photocatalytic efficiency of ZnO and TiO_2, Sol. Energy Mater. Sol. Cells 77 (2003) 65–82.
[8] Y.Z. Li, W. Xie, X.L. Hu, G.F. Shen, X. Zhou, Y. Xiang, X.J. Zhao, P.F. Fang, Comparison of dye photodegradation and its coupling with light-to-electricity conversion over TiO_2 and ZnO, Langmuir 26 (2010) 591–597.
[9] P.E. Jongh, E.A. Meulenkamp, D. Vanmaekelbergh, J.J. Kelly, Charge carrier dynamics in illuminated, particulate ZnO electrodes, J. Phys. Chem. B 104 (2000) 7686–7693.
[10] R. Comparelli, E. Fanizza, M.L. Curri, P.D. Cozzi, G. Mascolo, A. Agostiano, UV-induced photocatalytic degradation of azo dyes by organic-capped ZnO nanocrystals immobilized onto substrates, Appl. Catal. B 60 (2005) 1–11.
[11] L.W. Zhang, H.Y. Cheng, R.L. Zong, Y.F. Zhu, Photocorrosion suppression of ZnO nanoparticles via hybridization with graphite-like carbon and enhanced photocatalytic activity, J. Phys. Chem. C 113 (2009) 2368–2374.
[12] H.B. Fu, T.G. Xu, S.B. Zhu, Y.F. Zhu, Photocorrosion inhibition and enhancement of photocatalytic activity for ZnO via hybridization with C_{60}, Environ. Sci. Technol. 42 (2008) 8064–8069.
[13] Y.Z. Li, X. Zhou, X.L. Hu, X.J. Zhao, P.F. Fang, Formation of surface complex leading to efficient visible photocatalytic activity and improvement of photostability of ZnO, J. Phys. Chem. C 113 (2009) 16188–16192.

[14] T. Hirakawa, P.V. Kamat, Charge separation and catalytic activity of Ag@TiO_2 core–shell composite clusters under UV-irradiation, J. Am. Chem. Soc. 127 (2005) 3928–3934.
[15] P.D. Cozzoli, E. Fanizza, R. Comparelli, M.L. Curri, A. Agostiano, D. Laub, Role of metal nanoparticles in TiO_2/Ag nanocomposite-based microheterogeneous photocatalysis, J. Phys. Chem. B 108 (2004) 9623–9630.
[16] B. Xin, L. Jing, Z. Ren, B. Wang, H.G. Fu, Effects of simultaneously doped and deposited Ag on the photocatalytic activity and surface states of TiO_2, J. Phys. Chem. B 109 (2005) 2805–2809.
[17] Y. Zheng, L. Zheng, Y. Zhan, X. Lin, Q. Zheng, K. Wei, Ag/ZnO heterostructure nanocrystals: synthesis, characterization, and photocatalysis, Inorg. Chem. 46 (2007) 6980–6986.
[18] M.J. Height, S.E. Pratsinis, O. Mekasuwandumrong, P. Praserthdam, Ag-ZnO catalysts for UV-photodegradation of methylene blue, Appl. Catal. B 63 (2006) 305.
[19] W. Kubo, T. Tatsuma, Photocatalytic remote oxidation with various photocatalysts and enhancement of its activity, J. Mater. Chem. 15 (2005) 3104–3108.
[20] S. Bhattacharyya, A. Gedanken, Microwave-assisted insertion of silver nanoparticles into 3-d mesoporous zinc oxide nanocomposites and nanorods, J. Phys. Chem. C 112 (2008) 659–665.
[21] R.H. Wang, J. Xin, Y. Yang, H.F. Liu, L.M. Xu, J.H. Hu, The characteristics and photocatalytic activities of silver doped ZnO nanocrystallites, Appl. Surf. Sci. 227 (2004) 312–317.
[22] C.A.K. Gouvea, F. Wypych, S.G. Moraes, N. Duran, P. Peralta-Zamora, Semiconductor-assisted photodegradation of lignin, dye, and kraft effluent by Ag-doped ZnO, Chemosphere 40 (2000) 427–432.
[23] W.W. Lu, S.Y. Gao, J.J. Wang, One-pot synthesis of Ag/ZnO self-assembled 3D hollow microspheres with enhanced photocatalytic performance, J. Phys. Chem. C 112 (2008) 16792–16800.
[24] D. Lin, H. Wu, R. Zhang, W. Pan, Enhanced photocatalysis of electrospun Ag-ZnO heterostructured nanofibers, Chem. Mater. 21 (2009) 3479–3484.
[25] R. Georgekutty, M.K. Seery, S.C. Pillai, A highly efficient Ag-ZnO photocatalyst: synthesis, properties, and mechanism, J. Phys. Chem. C 112 (2008) 13563–13570.
[26] G. Shan, L.H. Xu, G.R. Wang, Y. Liu, Enhanced Raman scattering of ZnO quantum dots on silver colloids, J. Phys. Chem. C 111 (2007) 3290–3293.
[27] R.P. Wang, G. Xu, P. Jin, Size dependence of electron-phonon coupling in ZnO nanowires, Phys. Rev. B 69 (2004) 13303–13304.
[28] J.J. Wu, S.C. Liu, Catalyst-free growth and characterization of ZnO nanorods, J. Phys. Chem. B 106 (2002) 9546–9551.
[29] G.J. Exarhos, S.K. Sharma, Influence of processing variables on the structure and properties of ZnO films, Thin Solid Films 270 (1995) 27–32.
[30] G.I.N. Waterhouse, G.A. Bowmaker, J.B. Metson, Oxygen chemisorption on an electrolytic silver catalyst: a combined TPD and Raman spectroscopic study, Appl. Surf. Sci. 214 (2003) 36–51.
[31] G.J. Millar, J.B. Metson, G.A. Bowmaker, R.P. Cooney, *In situ* Raman studies of the selective oxidation of methanol to formaldehyde and ethene to ethylene oxide on a polycrystalline silver catalyst, J. Chem. Soc., Faraday Trans. 91 (1995) 4149.
[32] U.I. Avdeev, G.M. Zhidomirov, Ethylene and oxygen species adsorbed on a defect oxidized surface Ag(1 1 1)—theoretical analysis by DFT method, Surf. Sci. 492 (2001) 137–151.
[33] D. Beydoun, R. Amal, G.K.C. Low, S. Mcevoy, Novel photocatalyst: titania-coated magnetite. Activity and photodissolution, J. Phys. Chem. B 104 (2000) 1396–4387.
[34] P. Sagar, P.K. Shishodia, R.M. Mehra, H. Okada, A. Wakahara, A. Yoshida, Photoluminescence and absorption in sol–gel-derived ZnO films, J. Lumin. 126 (2007) 800–806.
[35] S. Fujihara, Y. Ogawa, A. Kasai, Tunable visible photoluminescence from ZnO thin films through Mg-doping and annealing, Chem. Mater. 16 (2004) 2965–2968.
[36] A.L. Rudd, C.B. Bresli, Photo-induced dissolution of zinc in alkaline solutions, Electrochim. Acta 45 (2000) 1571–1579.
[37] N. Kislov, J. Lahiri, H. Verma, D.Y. Goswami, E. Stefanakos, M. Batzill, Photocatalytic degradation of methyl orange over single crystalline ZnO: orientation dependence of photoactivity and photostability of ZnO, Langmuir 25 (2009) 3310–3315.
[38] A. Sclafani, J.M. Hermann, Influence of metallic silver and of platinum–silver bimetallic deposits on the photocatalytic activity of titania (anatase and rutile) in organic and aqueous media, J. Photochem. Photobiol. A 113 (1998) 181–188.
[39] J.G. Yu, Q.J. Xiang, M.H. Zhou, Preparation, characterization and visible-light-driven photocatalytic activity of Fe-doped titania nanorods and first-principles study for electronic structures, Appl. Catal. B 90 (2009) 595–602.
[40] K. Ishibashi, A. Fujishima, T. Watanabe, K. Hashimoto, Detection of active oxidative species in TiO_2 photocatalysis using the fluorescence technique, Electrochem. Commun. 2 (2000) 207–210.
[41] Q. Xiao, Z.C. Si, J. Zhang, C. Xiao, X.K. Tan, Photoinduced hydroxyl radical and photocatalytic activity of samarium-doped TiO_2 nanocrystalline, J. Hazard. Mater. 150 (2008) 62–67.
[42] T. Puangpetch, T. Sreethawong, S. Yoshikawa, S. Chavadej, Hydrogen production from photocatalytic water splitting over mesoporous-assembled $SrTiO_3$ nanocrystal-based photocatalysts, J. Mol. Catal. A 312 (2009) 97–106.
[43] Y. Ming, C.R. Chenthamarakshan, K. Rajeshwar, Radical-mediated photoreduction of manganese(II) species in UV-irradiated titania suspensions, J. Photochem. Photobiol. A 147 (2002) 199–204.